Zero Bias, Super Sensitive and Broadband UV Zero Bias, Super Sensitive and Broadband UV Photoconductor Based on Pt Nanoparticle Functionalized Ultrananocrystalline Diamond Nanowire Arrays

Rafael Velázquez,[1,2] Manuel Rivera,[2] Andrew F. Zhou,[3] David Bromley[2] and Peter X. Feng[1*]

1 Department of Physics, University of Puerto Rico, San Juan, PR 00936-8377, USA
2 Naval Air Warfare Center, Aircraft Division, Airborne Anti-Submarine Warfare Systems Engineering Division NAWCAD 4.5.14, 22268 Cedar Point Rd., Bldg. 2185 Rm 1160-A1, Patuxent River, MD 20670
3 Department of Physics, Indiana University of Pennsylvania, Indiana, PA 15705, USA

*** Authors to whom correspondence should be addressed; E-Mail: peter.feng@upr.edu**

ABSTRACT

The focus of the present work is the development of a broadband UV photodetector (PD) based on a superflat Boron doped ultrananocrystalline diamond (UNCD) nanowire (NW) arrays functionalized with Pt nanopartciles, wish is capable of withstanding high operating temperatures. The Pt nanoparticle functionalized UNCD NW arrays based photodetector exhibits an extremely large responsivity (1,224 A/W) to 300 nm light radiation at zero bias while taking advantage of diamond's unique stability as evidenced by its ability to function at temperatures as high as 200 ^{o}C Additionally, the investigated PD has a fast response time as short as 17 ms.

Introduction

Current needs in applications such as space exploration and Earth's surface incident radiation monitoring have imposed new requirements on the next generation of deep UV detectors. In particular, reduced energy consumption, enhanced resistance to the performance degradation at high temperatures and high portability appear to be extremely important properties for a growing demand of crucial applications[1]. Recent progress has been made towards achieving these goals. Several nanostructured wide bandgap materials based detectors have been developed[2,3,4]. However, designing a multi-functional material simultaneously exhibiting desired properties in PDs still remains a challenge.

With this in mind, we aim at creating a cost-effective, high-performance UNCD based UV PD that satisfies the market needs of high-temperature and self-power operation. Diamond has attracted significant interest as a promising candidate for UV sensing applications due to its wide bandgap, chemical stability and robustness. Diamond also has excellent mechanical hardness and tunable band-gap via doping[5,6]. The undoped single-crystal diamond has a band-gap of 5.5eV[7,8]. Lansley and his group used natural and synthetic diamond to achieve a very fast time response (less than microsecond) when these detectors were radiated with pulsed laser beams[9]. Pace and his group used both single crystalline and polycrystalline diamond films to develop two types of photoconductive detectors[10]. The obtained experimental data suggested that single crystalline diamond based detectors had much higher sensitivity than the PD using polycrystalline diamond [11,12].

However, natural single crystalline diamond is very expensive, whereas either nanocrystalline diamond (NCD) or micropolycrystalline diamond (MCD) films have rough surfaces, with which no precise nanostructures for electronic devices can be made. In contrast, UNCD has excellent film thickness uniformity with extremely low surface roughness independently of its film thickness. Furthermore, UNCD can be obtained from a reliable and cost-effective production method which yields consistent UNCD material properties. Our research presented in this paper focuses on the functionalization of superflat ultrananocrystalline diamond (UNCD) material with

Pt nanoparticles from which nanowire arrays have been fabricated for the development of novel self-powered UV PD devices.
The rationale for the work is based on the fact that Pt nanoparticle functionalized UNCD NW based photodetectors would drastically improve the response times because of their large surface-to-volume ratios, one-dimensional nanostructures UNCD NW with Pt particles in the surface of the NWs are an essential block to fabricate a field-effect transistor (FET).
It is expected the Pt on the surface of the NWs may change the conductance by changing the surface charges and states, this changes the gate potential, the work function and band alignment, resulting in a gate coupling, and a change in carrier mobility. All of these will be regarded as a floating gate effect on the conducting channel of the FET. The strong local electric field at the reversely biased Schottky barrier area will quickly separate the photon-generated electrons and holes, which reduces the electron-hole recombination rates, this reduce the power consumption, increase the portability and enhance the signal-to-noise ratio[13]. The obtained experimental data clearly indicates that the newly designed PD exhibits high photocurrent and outstanding responsivity to both UVB and UVC radiations at zero applied voltage while taking advantage of diamond's unique stability as evidenced by its ability to function at temperatures as high as 300 ^{o}C. Additionally, the investigated PD has fast response times of less than 17 ms. Few materials reported so far, if any, possess such a desirable set of UV sensing performance characteristics.

SYNTHESIS

The boron-doped UNCD thin film were synthesized by Advanced Diamond Technologies, Inc. The UNCD films were synthesized with the microwave plasma chemical vapor deposition (MPCVD) system (Lambda Technologies Inc.), using a standard deposition procedure. The UNCD films were grown at a substrate temperature of 760 ^{o}C, a microwave power of 2100 Watts, and an $Ar/CH_4/H_2$ gas mixture with flow rates of 400/1.2/8 s.c.c.m, respectively. Throughout the UNCD deposition, the chamber pressure was maintained at 120 mbar. The UNCD growth procedure was performed on a silicon wafer substrate for 1 hour which resulted in an 80 nm thick UNCD film deposition. As a source of boron was use Trimethylboron (TMB, i.e., B(CH3)3) for the doping. For More details regarding the synthesis process of UNCD growth and doped process are described elsewhere[14,15,16,17].

UNCD nanowire (70 nm in width and 35 μm in length) arrays were then fabricated by using top-down based lithography techniques. A detailed description of the crystalline structure and surface morphology characterization, electron beam lithography and nanowire array fabrication can be found in the references[11,12,18].

Finally, using a sputtering method 10 nm Aluminum/100 nm platinum pair were deposited as electrodes (Ohmic contacts) onto two sides of the UNCD nanowire arrays and in the process Pt nanoparticles was functionalize on the surface of UNCD nanowires resulting in individual punctual Schottky contacts in surface of the NW . The fabricated nanowire device was then annealed at 150 ^{0}C for 5 minutes in the probe station chamber with a LakeShore temperature controller.

It should be mentioned that at zero bias, no induced photocurrent could be detected from the two Ohmic contact based PD exposed to deep UV light radiation. It was also noticed that the carrier transport of UNCD relied on hopping transport mechanisms resulted in a low carrier velocity. In other words, the UNCD films based PDs had very poor performance. Therefore, very few groups work on it even though UNCD is much cheaper than single crystal diamond. In the present paper, Pt nanoparticles have been used to functionalize the surface of UNCD nanowires in

an attempt at improving the performance of a UNCD based PD. The prototype forms a non-symmetrical Schottky contact device containing a Schottky barrier (SB) contact at one side of the device and an ohmic contact at the other side for each Pt nanoparticle on the UNCD wire surface. The entire device can be regarded as a nanowire connected in series with a SB diode (one for each Pt nanoparticle). The Schottky contact area in each wire constitutes the bottleneck for the current transport in the device. The original SB height φ_{SB} is determined by the work-function difference between the metal and Pt nanoparticles on the surface of the UNCD wires and the interface states. The current passing through the Schottky contact is very sensitive to the Schottky barrier height and barrier width. Light irradiation at or near the SB area can change the local electric-field distribution, and thus cause the variations of the SB height and width, resulting in a detectable current change[13,19].

Images

Figure 1a shows the SEM image of the fabricated UNCD NWs with a length of nearly 35 μm, which are connected to the Al/Pt electrodes. The gap is approximately 1 μm between the UNCD NWs. Figure 1b shows an enlarged SEM image of a typical single wire, from which one may estimate that each wire consists of tiny UNCD nanoparticles with a diameter of about 5-7 nm. A detailed characterization of the UNCD with a high resolution transmission electron microscope can be found in our previous reports[11,12]. The UNCD NWs have an average width of 70 nm.

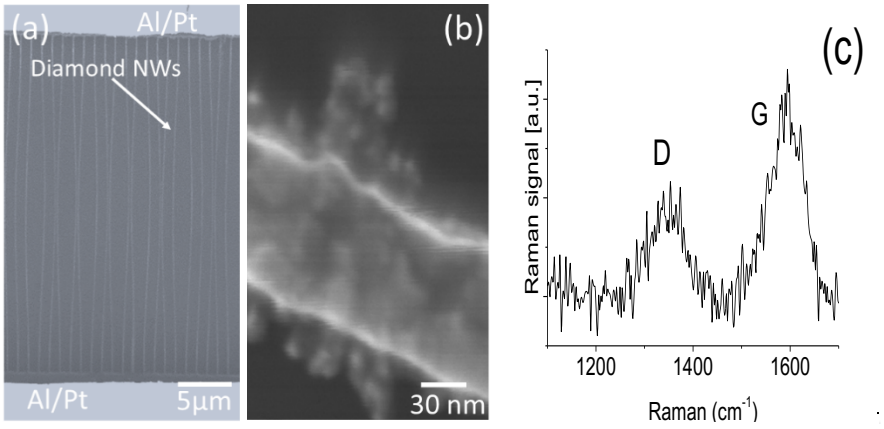

Figure 1 (a) SEM image of the UNCD nanowire array, (b) an enlarged image of a single UNCD NW, and (c) a typical Raman spectrum of the boron-doped UNCD wire array.

Raman Spectroscopy

Raman scattering is a powerful, semi-quantitative method to examine the diamond structure because the sp^2 and sp^3 carbon bondings are very sensitive to Raman scattering. Figure 1c shows a typical Raman spectrum of the boron (B)-doped UNCD wire arrays by using a triple monochromator with an excitation wavelength of 514 nm from an Ar^+ ion laser and a microscope to focus the laser beam onto the NWs. Two broad bands at 1332^{-1} cm and 1595^{-1} cm, respectively, are clearly visible that have been assigned to the regular D band and G band. Normally, the G band is from the sp^2 carbon bonds, indicating the synthesized sample is a carbon mixed UNCD material. The broad Raman spectral intensity taken at the D band (1332 cm^{-1}) from sp^3 carbon bonds proves

that the material is indeed diamond. Broadened profile of the D band could be related to the polycrystalline structure of randomly oriented grains or the nano-scale effect[20].

Prototype

To understand the electrical properties, the fabricated UNCD NWs were connected to a basic electric circuit to form the prototype. Fig. 2 shows a schematic diagram of the prototypical photodetector. Two external conductive electrodes installed at two ends of UNCD nanowires were serially connected to a precision resistor $R_{precise}$, a switcher, and a step-up/step-down voltage regulator V_o (Keysight E3643A power supply). The set-up also consisted of two HEWLETT 34401A programmable electronic multimeters (V_1 and V_2) monitored by a Labview program, from which the variations of the two voltages ($V_{prototye}= V_2 -V_1$) and the current ($I_{prototype}=V_1/R_{precise}$) in the prototype were recorded. A tungsten filament and a thermocouple were used as a controllable heater for obtaining a desired operating temperature.

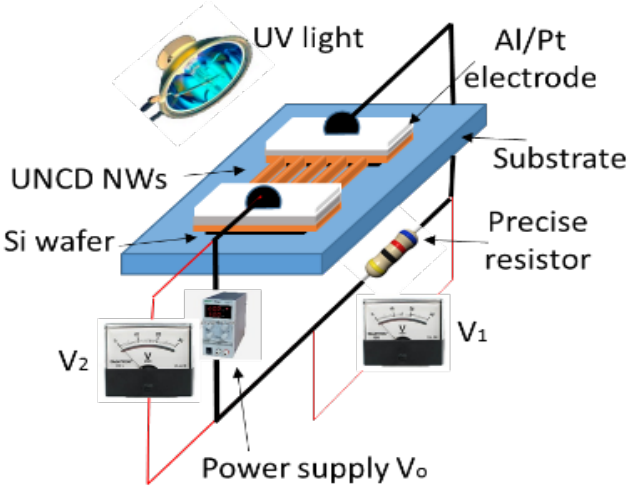

Figure 2 Schematic setup of the prototype.

Electrical Properties

Even though one of the focuses of the present work is the ability of the PD to operate at zero bias and for this case V_2=0, it is still necessary to understand how the bias affects the properties of the UNCD nanowires based detector. Typical responses at different reverse biases are shown in Fig. 3. In Figure 3a we can see that the fabricated photodetector displays a quick, well-defined response. A higher bias voltage yields a higher induced photocurrent and a larger responsivity (ratio between the output photocurrent and the input UV light power). As seen in Figure 3a, the obtained photocurrents (I_{ph}) at -1, -2 and -2.5 V bias are approximately 6, 14 and 29 times larger, respectively, than that at zero bias. This characteristic is much better than that of the reported SiC, diamond and other oxide semiconductors based detectors, although the measures were taken at higher bias[21,22,23,24]. Furthermore, a fast response time and recovery time were also observed regardless of the applied bias.

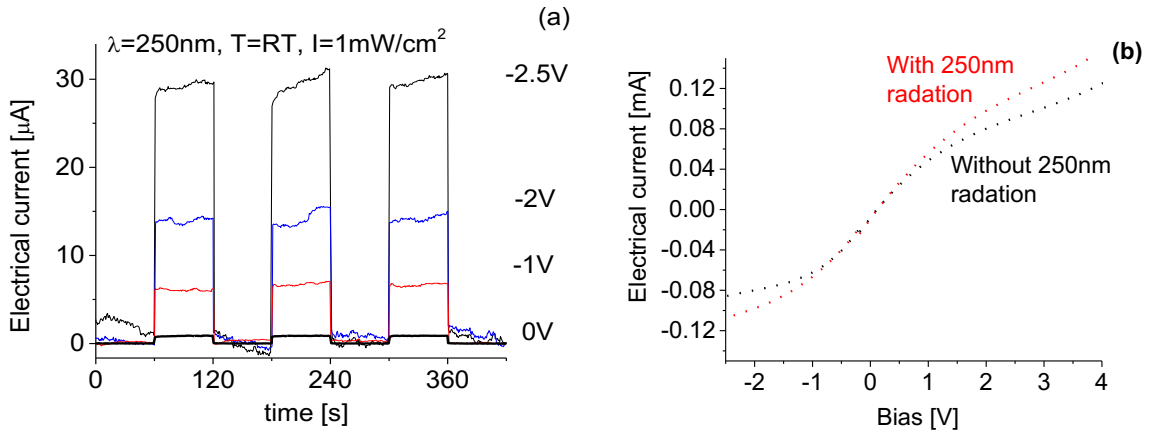

Figure 3 (a) Bias effect on the response when UNCD NWs based photodetector was cycled with a period of 2 minutes between the "switch-on" and "switch-off" of the 250 nm UV light radiation at room temperature, and (b) the electrical current as a function of bias with and without UV radiation.

A slight variation of the baseline was also observed in Fig. 3a, as the reverse bias from the power supply was increased. Following an increase of bias magnitude the dark current unavoidably increased as well as the noise level. Therefore, the signal-to-noise ratio did not improve significantly as the bias magnitude was increased. Fig 3b shows the typical current-voltage reverse bias characteristics in dark and 250nm UV light at room temperature. Nonlinear current-voltage curve was observed at applied bias, which indicates a Schottky diode behavior of the NWs/Pt contacts.

Characterization Responsivity

When the photodetector is exposed to UV light, the photonic energy is absorbed by the valence electrons, which leads to the induced photocurrent. Three different UV wavelengths were used for characterizing the responsivity of the boron doped UNCD NWs. The intensity of the UV light onto the surface of the photodetector was controlled by shifting the height between the UV light source and the detector. Fig. 4 illustrates typical photoresponses of the fabricated UV photodetector to 250, 300 and 350 nm UV light illuminations, respectively, subjected to the on/off cycles with a period of 120 seconds. Results of the UV photodetector presented in Fig. 4 were tested at room temperature under three different incident radiation intensities.

Fig. 4a shows the photoresponses at zero bias and room temperature when the prototype is exposed to 250 nm light illumination cycling with a period of 120 seconds. When the detector was exposed to UV light radiation, the induced photocurrent quickly increased and reached a stable maximum value. When the UV radiation was switched off, the photocurrent decreased to zero value. Excellent features in repeatability and stability are clearly visible. The induced photocurrent can be attributed to the absorption of UV photons by the active UNCD NWs material. A decrease in photocurrent magnitude as the intensity of UV light reaching the surface of the PD decreases is expected. However, no significant change in photocurrent was observed when the UV intensity ranged from 1 mW/cm^2 to 0.03 mW/cm^2, indicating that the detector might be saturated with UV

radiation. Under such condition, the generated photocurrent from the UV photodetector reached 0.94 μA. Since the average length and width of each nanowire is 35 nm and 70 nm and the total number of nanowires in the platform is 100, we estimate a total exposure area of 245 μm^2 for the present prototype. Consequently, we obtained a responsivity around 406 A/W for 300nm UV light .This value is at least three orders of magnitude higher than what has been reported so far on zero bias or self-powered deep UV photodetectors made of different materials[3,4,15].

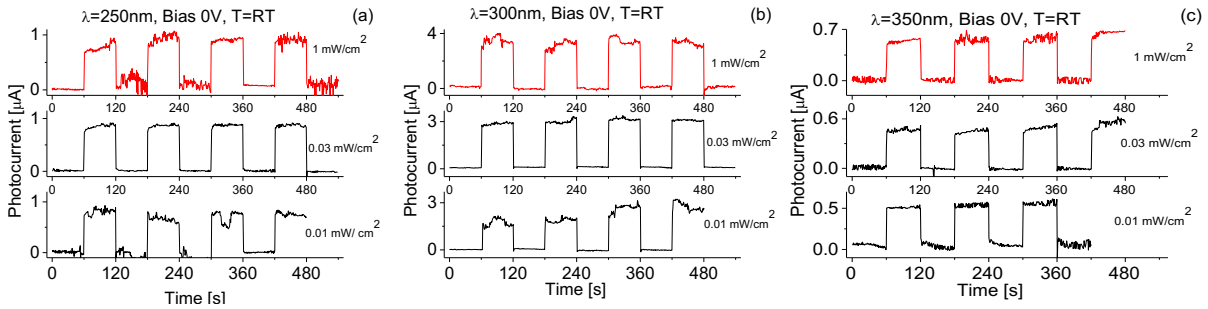

Figure 4 Time-dependent photoresponsivity at zero bias and room temperature when the prototype was on/off cycled with a period of 120 seconds under (a) 250 nm, (b) 300 nm, and (c) 350 nm light radiations at different intensities.

Similar phenomena including good repeatability and stable baseline were also observed when the photodetector was exposed to 300 nm of UV light illumination as shown in Fig. 4b. The main observed difference is that the 300 nm induced photocurrent was almost 3 times larger than that induced with 250 nm light illumination. As a result, an extremely high responsivity up to 1,224 A/W was obtained from the present photodetector when exposed to 300 nm light.

It should be mentioned here that the total size of the platform used in the present case is only 0.5 mm^2, which is much smaller than those UV detectors reported by others. From the literature it is also noticed that several groups were successful in achieving very high responsivity from nanomaterials based photodetectors in the UV region at a high applied bias. This has the disadvantage of increasing dark current level, resulting in a poor signal-to-noise ratio. Furthermore, either size or weight of a bias based detector could not be reduced easily due to the power supply constraint. In contrast, the self-power zero bias PDs tend to exhibit low dark current magnitudes[25,26,27,28,29]. In the present case, for example, the obtained dark current is only 2×10^{-7} A. Since the induced current is 3.5 μA, we have a signal-to-noise ratio of 18. Because it does not require an external power supply, the detector can be much smaller. The miniaturization of PD devices is extremely important for a wide number of space applications.

Characterizations of the time-dependent photoresponsivity of the fabricated detector at zero bias and room temperature, when exposed to 350 nm light illumination were also carried out and the results are shown in Fig. 4c. Excellent repeatability and stability, as well as quick response time, are still clearly visible. However, the obtained 350 nm light-induced photocurrent is almost 6 times less than that induced by 300 nm light. Correspondingly, a responsivity of 244 A/W related to 350 nm radiation was obtained.

As shown in Fig 4, the responsivity of the present boron-doped UNCD based PD is highly related to the wavelength of UV light radiation. The highest responsivity of 1,224 A/W is related to the 300 nm UV light illumination. Applying Mendoza's model to the obtained relationship between

the responsivity strength and the wavelength of UV light radiation, it was estimated that the present boron-doped UNCD has a band-gap energy around 4.1 eV (~ 300 nm)[30]. This result is in good agreement with the previous studies of the bandgap shift obtained from the basic characterization of UNCD[31,32].

Temperature Effect

The photoresponse of the UNCD based UV sensor was also studied at different operating temperatures. The results, presented in Fig. 5, were conducted with a 250 nm wavelength UV light radiation. The vast majority of UV PDs reported up to date, have proven to be inoperable at temperatures above 100 to 150 ^{o}C[23]. As shown in Fig. 5, the UNCD based PD continues to perform well above this temperature limit. Comparison of the responses obtained at room temperature Fig. 4 with that at higher temperatures Fig. 5 reveals that the photocurrent decreases with the increase of the temperature. This, as well as a decrease in signal-to-noise ratio, is expected due to the unavoidable increase in dark current and thermal noise as the temperature increases. However, as shown in Fig. 5, the UNCD prototype maintains an excellent repeatability and stability as operating temperature is increased up to 100 ^{o}C. Additionally, it was observed that the photodetector under investigation was capable of withstanding operating temperatures as high as 200 ^{o}C while retaining a clear, stable and reproducible signal well above the thermal noise threshold. Further increasing the temperature to 300 ^{o}C, the light induced photocurrent response from the PD is still measurable even though the thermal noise contribution was large. This is a considerable increase in PD heat tolerance compared to the majority of UV sensors reported so far and it is directly attributed to the intrinsic properties of diamond.

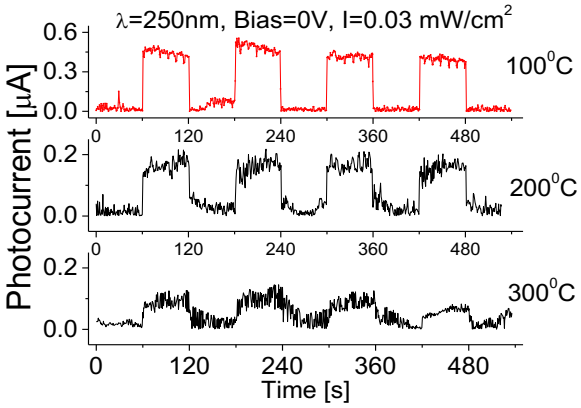

Figure 5 Temperature effect on the photoresponse of the UV photodetector when exposed to 250 nm light.

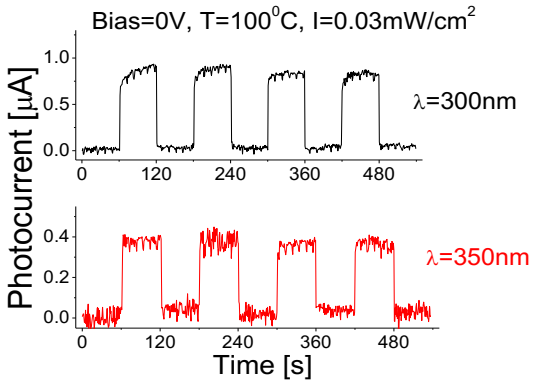

Figure 6 Temperature effect on the responsivity of the UV photodetector to 300 nm and 350 nm light when operated at 100 ºC.

Similar results for the PD prototype under investigation were obtained upon exposition to 300 and 350 nm radiations. As seen in Fig. 6, at an operating temperature of 100 ºC the UNCD based photodetector experiences a slight decrease in photocurrent compared with its room temperature performance, but the signal-to-noise ratio is still significantly high, and the fast response times were not affected. Also, at an operating temperature of 100 ºC, the PD prototype still exhibits high responsivity values when exposed to 250, 300 and 350 nm radiations.

Response Time and Recovery Time

As previously mentioned, the UNCD based PD exhibited fast response and recovery times regardless of the incident radiation at operating temperatures up to 200 ºC. To further investigate the characteristic response and recovery times (t_{res} and t_{rec}) of the prototype, high time-resolution measurements were performed. Determination of the t_{res} values was based on the time interval for the photocurrent to rise to 90% of its peak value and t_{rec} as the time interval for the signal to decay to 10% of its peak value.

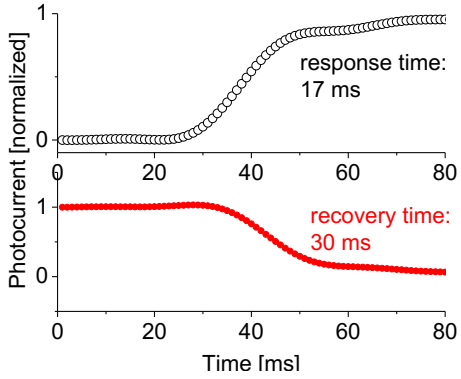

Figure 7 Response time and recovery time of the boron-doped UNCD based UV photodetector when the 250 nm light illumination is turned on and off at room temperature.

In Fig. 7, the typical measurements of both t_{res} and t_{rec} are shown upon switching on or off the 250 nm UV light source. As shown in Fig. 7, the PD under investigation exhibits a response time of 17

ms. On the other hand, t_{rec} was found to be around 30 ms; almost twice the response time t_{res}. This is likely due to the intrinsic radiation intensity decay of the light source as it is switched off. Even though the obtained rise and decay times of the UNCD based PD can't be comparable to those of the reported single crystalline diamond based PD, the present UNCD NW based still shows it advantages including cost-effective, self-powered feature, and higher responsivity. Nevertheless, the obtained response times are still much faster than most reported PDs with similar responsivity values[33,34].

Conclusion

Based on the superflat surface synthesized UNCD boron-doped film, a precise UNCD nanowire array has been designed and fabricated. To the best of our knowledge, this is the first demonstration of the zero bias solar-blind photodetectors based on Pt nanoparticle functionalized boron-doped UNCD nanowire arrays, which provide ultra-high responsivities up to 406 A/W, 1,224 A/W and 244 A/W at 250 nm, 300 nm and 350 nm UV wavelengths, respectively. The newly developed PD possesses outstanding features in quick response (less than 17 ms), excellent repeatability and stability. Experimental data also show that an extremely large responsivity can be achieved with a high reverse bias. The obtained photocurrents are almost 6, 14, 29 times larger at -1, -2 and -2.5 V bias, respectively, than that at zero bias. These characteristics are much better than those reported of SiC, diamond and other oxide semiconductors based zero bias solar-blind photodetectors. In addition, the photodetector based on UNCD NW arrays performs extremely well even at temperatures as high as 200°C, making the UNCD NW array arrangement an ideal candidate for UV sensing applications in harsh environments.

Acknowledgments
This work is financially supported by NSF-CREST Center for Innovation, Research and Education in Environmental Nanotechnology (CIRE2N) Grant Number HRD-1736093. Manuel Rivera gratefully acknowledges NASA fellowship support through the NASA Grant NNX15AI11H. Andrew Zhou gratefully acknowledges the IUP Senate Fellowship Grant.

References

1. Wang, Z. L., Self-Powered Nanosensors and Nanosystems. *Adv. Mat*. **24** (2) 280-285 (2012).
2. Hao, L. Z., Liu, Y. J., Gao, W., Han, Z. D., Xu, Z. J., Liu, Y. M. & Zhu, J. Self-powered photosensing characteristics of amorphous carbon/silicon heterostructures. *RSC Adv.* **6** (46) 40192-40198 (2016).

3. Chen, H., Yu, P., Zhang, Z., Teng, F., Zheng, L., Hu, K. & Fang, X. Ultrasensitive Self-Powered Solar-Blind Deep-Ultraviolet Photodetector Based on All-Solid-State Polyaniline/MgZnO Bilayer. *Small*.**12** (42) 5809-5816 (2016).

4. Tsai, D., Lien, W., Lien, D., Chen, K., Tsai, M., Senesky, D. G., Yu, Y., Pisaro, A. P. & He, J. Solar-Blind Photodetectors for Harsh Electronics. *Sci. Rep*. **3** 2628 (2013).
5. Ashfold, M. N. R., May, P. W., Rego, C. A. & Everitt, N. M. Thin film diamond by chemical vapour deposition methods Chemical Society Review **23** 21-30 (1994).
6. Chen, Q., Gruen, D. M., Krauss, A. R., Corrigan, T. D., Witek, M. & Swain, G. M.

The structure and electrochemical behavior of nitrogen-containing nanocrystalline diamond films deposited from CH4/N2/Ar mixtures. Journal of The Electrochemical Society **148** E44-51 (2001).
7. Liua, Z., Ao, J-P., Lia, F., Wanga, W., Wangd, J., Zhanga, J. & Wanga, H-X. Photoelectrical characteristics of ultra thin TiO_2/diamond photodetector. *Materials Letters.* **188** 52–54 (2017).

8. Balducci, A., Marinelli, M., Milani, E., Morgada, M. E., Tucciarone, A., Verona-Rinati G., Angelone, M. & Pillon, M. Extreme ultraviolet single-crystal diamond detectors by chemical vapor deposition. *Appl. Phys. Lett*. **86** 193509 (2005).

9. Lansley, S. P., Betzel, G. T., Metcalfe, P., Reinisch, L. & Meyer, J. Comparison of natural and synthetic diamond X-ray detectors. *Australas Phys Eng Sci Med*. **33**(4):301-6 **(**2010**).**

10. Pace, E. & De Sio, A. Innovative diamond photo-detectors for UV astrophysics. *Mem. S.A.It. Suppl.* **14** 84-89 (2010).
11. Roberson, J. *et al.* Diamond-like Amorphous Carbon. *Mater. Sci. Eng. R-Pep*. **37** (4-6) 129-281 (2002).
12. Piazza, F., Gonzalez, J. A., Velazquez, R., De Jesus, J., Rosario, S. A. & Morell, G. Diamond Film Synthesis at Low Temperature. *Diamond Relat. Mater.* **15** (1) 109-116 (2006).

13. Hu, Y., Zhou, J., Yeh, P. H., Li, Z., Wei, T. Y. & Wang, Z. L. Supersensitive, Fast-Response Nanowire Sensors by Using Schottky Contacts. *Adv. Mater*. **22** 3327–3332 (2010).

14. Zeng, H., Arumugam, P., Siddiqui, S. & Carlisle J. Low temperature boron doped diamond. Applied Physics Letters **102** 223108 (2013).

15. Wang, X. Synthesis, Fabrication, Characterization and Application of Ultranano Crystalline Diamond Micro and Nanostructures. Ph.D. Thesis, Physics Department, University of Puerto Rico, San Juan, PR, **2012**.
16. Wang, X., Ocola, L. E., Divan, R. S. & Sumant, A. V. Nanopatterning of Ultrananocrystalline Diamond Nanowires. *Nanotechnology*. *Nanotechnology*. **23** (7) 1-7 (2012).
17. Zeng, H., Konicek, A., Moldovan, N., Mangolini, F., Jacobs, T., Wylie, I., Arumugam, P., Siddiqui, S., Carpick, R. & Carlisle, J. Boron-doped ultrananocrystalline diamond synthesized with an H-rich/Ar-lean gas system. *Carbon,* **84** 103–117 (2015).
18. Auciello, O. & Sumant, A. V. Status review of the science and technology of ultrananocrystalline diamond (UNCD™) films and application to multifunctional devices. *Diamond Relat. Mater.* **19** (7-9) 699-718 (2010).

19. Lee, C. H., Qin, S., Savaikar, M. A., Wang, J., Hao, B., Zhang, D., Banyai, D., Jaszczak, J. A., Clark, K. W., Idrobo, J-C., Li, A-P. & Yap, Y. K. Room-temperature tunneling behavior of boron nitride nanotubes functionalized with gold quantum dots. *Adv. Mater*. **25** 4544 (2013).

20. Tsujimoto, Y., Matsushita, Y., Yu, S., Yamaura, K. & Uchikoshi, T. Size Dependence of Structural, Magnetic, and Electrical Properties in Corundum-type Ti2O3 Nanoparticles Showing Insulator-Metal transition . *Journal of Asian Ceramic Societies*, **3**(3) 325–33 (2015).

21. Velázquez, R. Aldalbahi, A., Rivera, M. & Feng, P. Fabrications and Application of Single Crystalline GaN for High-Performance Deep UV Photodetectors. *AIP Adv*. 6 085117-1-12 (2016).

22. Rivera, M., Velázquez, R., Aldalbahi, A., Zhou, A. F. & Feng, P. Self-Powered 2D Boron Nitride Nanosheets Based Broadband UV Photodetectors for Hazardous Environments. *Sci. Rep*. **7** 42973 (2017).
23. Aldalbahi, A., Li, E., Rivera, M., Velazquez, R., Altalhi, T., Peng, X. & Feng, P. A New Approach for Fabrications of SiC Based Photodetectors. *Sci. Rep*. **6** 23457 (2016).
24. Peng, L., Hu, L. & Fang, X. Low-Dimension Nanostructure Ultraviolet Photodetector. *Adv. Mater*. **25** 5321-5328 (2013).
25. Hu, P., Wang, L., Yoon, M., Zhang, J., Feng, W., Wang, X., Wen, Z., Idrobo, J. C., Miyamoto, Y. & Geohegan, D. B. Highly Responsive Ultrathin GaS Nanosheet Photodetectors on Rigid and Flexible Substrates. *Nano letters.* **13**(4) 1649-1654 (2013).
26. Yang, S., Li, Y., Wang, X., Huo, N., Xia, J-B., Li, S-S. & Li, J. High performance few-layer GaS photodetector and its unique photo-response in different gas environments. *Nanoscale.* **6** (5) 2582-2587 (2014).
27. Hu, L., Yan, J., Liao, M., Xiang, H., Gong, X., Zhang, L. & Fang, X. An optimized ultraviolet-a light photodetector with wide-range photoresponse based on ZnS/ZnO biaxial nanobelt *Advanced Materials.* **24**(17) 2305-2309 (2012).
28. Wu, J., Koon, G. K. W., Xiang, D., Han, C., Toh, C. T., Kulkarni, E. S., Verzhbitskiy, I., Carvalho, A., Rodin, A. S. & Koenig, S. P. Colossal Ultraviolet Photoresponsivity of Few-Layer Black Phosphorus. *ACS Nano*. **9**(8) 8070-8077 (2015).
29. Li, L., Lee, P. S., Yan, C., Zhai, T., Fang, X., Liao, M., Koide, Y., Bando, Y. & Golberg, D. Ultrahigh-Performance Solar-Blind Photodetectors Based on Individual Single-crystalline $In_2Ge_2O_7$ Nanobelts. *Adv. Mat*. **22** (45) 5145-5149 (2010).
30. Mendoza, F., Makarov, V., Weiner, B. & Morell G Solar-Blind Field-Emission Diamond Ultraviolet Detector. Appl. Phy. Lett. **107** 201605-1-5 (2015).
31. Sankaran, K. J., Panda, K., Sundaravel, B., Chen, H-C., Lin, I-N., Lee, C-Y. & Tai, N-H. Engineering the Interface Characteristics of Ultrananocrystalline Diamond Films Grown on Au-Coated Si Substrates. *ACS Appl. Mater. Interfaces*, **4** (8) pp 4169–417 (2012).
32. Franta, D., Zajíčková, L. Karásková, M., Jašek, O., Nečas, D., Klapetek, P. & Valtr, M. Optical characterization of ultrananocrystalline diamond films. *Diamond & Related Materials*, 17 1278–1282 (2008).
33. Dhanabalan, S. C., Ponraj, J. S., Zhang, H. & Bao, Q. Present Perspectives of Broadband Photo-Detectors Based on Nanobelts, Nanoribbons, Nanosheets and the Emerging 2D Materials. *Nanoscale*. **8** (12) 6410-6434 (2016).
34. Feng, P., Wang, X., Aldalbahi, A. & Zhou, A. F. Methane Induced Electrical Property Change of Nitrogen Doped Ultrananocrystalline Diamond Nanowires. *Appl. Phys. Lett*. **107** (23) 233103 (2015).